

Lowest Two $T = \frac{3}{2}$ States of ^{17}F Observed in the $^{16}\text{O}(p,p)^{16}\text{O}$ Reaction*

J. R. PATTERSON, H. WINKLER, AND C. S. ZAIDINS†

California Institute of Technology, Pasadena, California

(Received 14 July 1967)

The lowest $T = \frac{3}{2}$ state of ^{17}F has been observed in the isospin-forbidden $^{16}\text{O}(p,p)^{16}\text{O}$ reaction, where anomalies have been found in the elastic channel and in the inelastic channels to the 6.13- and 7.12-MeV states of ^{16}O . The partial width Γp_0 of this state as obtained from a phase-shift analysis of the elastic data is $\Gamma p_0 = (40_{-20}^{+10})$ eV. The excitation energies of both the lowest and the next higher $T = \frac{3}{2}$ states have been determined by using the $^{12}\text{C}(\alpha,n)^{16}\text{O}$ threshold and a $^{24}\text{Mg}(\alpha,\gamma)^{28}\text{Si}$ resonance as calibration points. Values of $E_x = 11.202 \pm 0.008$ MeV ($E_p = 11.276 \pm 0.008$ MeV) and 12.554 ± 0.008 MeV ($E_p = 12.714 \pm 0.008$ MeV) have been obtained, in agreement with the positions determined from the $^{15}\text{N}(^3\text{He},n)^{17}\text{F}$ reaction. The second $T = \frac{3}{2}$ state is well suited as an energy calibration point for accelerators.

I. INTRODUCTION

A NUMBER of higher isospin states in light nuclei have been located recently by isospin-allowed reactions such as $(^3\text{He},n)$,^{1,2} $(^3\text{He},p)$,^{3,4} and (p,t) and $(p,^3\text{He})$,⁵ where they may be populated selectively because of their structural properties. In some of the reactions cited, spin and parity measurements have come from analysis of the angular distributions. Measurements on the states as compound-nuclear resonances can give useful complementary information such as widths.⁶⁻⁸

In ^{17}F , the second and third $T = \frac{3}{2}$ states were found by Hardie, Dangle, and Oppliger⁹ as narrow anomalies at 12.671- and 13.215-MeV bombarding energy, respectively, in the elastic scattering of protons from an oxygen-gas target. No anomaly was observed to correspond to the expected position of the first $T = \frac{3}{2}$ state. The missing state was located recently by Adelberger and Barnes² in the isospin-allowed $^{15}\text{N}(^3\text{He},n)^{17}\text{F}$ reaction. With accurate information on the position of the state, a new search was undertaken in the $^{16}\text{O}(p,p)^{16}\text{O}$ reaction, extending to the inelastic scattering since theoretical estimates¹⁰ of the two-particle-one-hole

structure of the state would favor proton emission to the 3^- , 1^- , and 2^- excited states of ^{16}O . After the state was found, the anomalies were measured at several angles and the position and width determined, together with the position of the second $T = \frac{3}{2}$ state.

II. EXPERIMENT

The lowest $T = \frac{3}{2}$ state of ^{17}F was observed in two types of measurement: (1) With a silicon monoxide foil less than 1-keV thick as a target, the scattered protons were observed in a 61-cm double-focusing magnetic spectrometer. (2) A differentially pumped oxygen-gas target was used and the scattered protons observed in solid-state counters. The second $T = \frac{3}{2}$ state was observed only in the elastic scattering of protons by using a thin SiO target and solid-state counters. In each case, the ONR-CIT tandem accelerator was carefully adjusted for the best possible energy homogeneity of the beam. Slit openings between 0.7 and 1.2 mm were used at the 90° magnetic analyzer ($r = 86$ cm) of the tandem. In order to minimize beam energy fluctuations, a signal display from the tandem terminal pickup plate was used to set the corona stabilizer gain control to its optimum value. The beam current was in the range 0.1–0.5 μA .

A. Measurement of the Scattering Anomalies of the First $T = \frac{3}{2}$ State

(1) To maintain a uniform target potential, a thin gold layer (about $8 \mu\text{g cm}^{-2}$) was evaporated onto the self-supporting silicon monoxide target foils, the foil thickness being approximately $20 \mu\text{g cm}^{-2}$ SiO. The elastic and all inelastic groups up to p_4 could be fully resolved with the 1.27-cm counter slit employed in the focal plane of the spectrometer. However, this slit opening was still wider than the full width of a particular group in the focal plane, as caused by the beam energy spread, target thickness, and $dE/d\theta$ of the scattered particles. A foil was used in the focal plane to separate α particles from protons. Anomalies were found in the p_2 and p_4 excited state groups at 150° (lab) and a smaller anomaly was suggested in the elastic scattering.

* Supported in part by the U. S. Office of Naval Research [Nonr-220(47)].

† Present address: University of Colorado, Boulder, Colorado.

¹ E. G. Adelberger and C. A. Barnes, *Bull. Am. Phys. Soc.* **10**, 1195 (1965).

² E. G. Adelberger and C. A. Barnes, *Phys. Letters* **23**, 474 (1966).

³ D. C. Hensley and C. A. Barnes, *Bull. Am. Phys. Soc.* **10**, 1194 (1965).

⁴ B. Lynch, G. M. Griffiths, and T. Lauritsen, *Nucl. Phys.* **65**, 641 (1965); G. M. Griffiths, *ibid.* **65**, 647 (1965).

⁵ J. Cerny, R. H. Pehl, G. Butler, D. G. Fleming, C. Maples, and C. Detraz, *Phys. Letters* **20**, 35 (1966); G. T. Garvey, J. Cerny, R. H. Pehl, *Phys. Rev. Letters* **12**, 726 (1964).

⁶ D. J. Bredin, O. Hansen, G. M. Temmer, and R. Van Bree, *Isobaric Spin in Nuclear Physics*, edited by J. D. Fox and D. Robson (Academic Press Inc., New York, 1966), p. 472.

⁷ M. J. LeVine and P. D. Parker, *Bull. Am. Phys. Soc.* **12**, 51 (1967); H. M. Kuan and S. S. Hanna, *Phys. Letters* **24B**, 566 (1967).

⁸ F. S. Dietrich, M. Suffert, S. S. Hanna, and A. V. Nero, in *Proceedings of the International Conference on Nuclear Physics, Gallinburg, Tennessee, 1966* (Academic Press Inc., New York, 1967); and *Phys. Rev.* (to be published).

⁹ G. Hardie, R. L. Dangle, and L. D. Oppliger, *Phys. Rev.* **129**, 353 (1963).

¹⁰ B. Margolis and N. de Takacsy, *Can. J. Phys.* **44**, 1431 (1966).

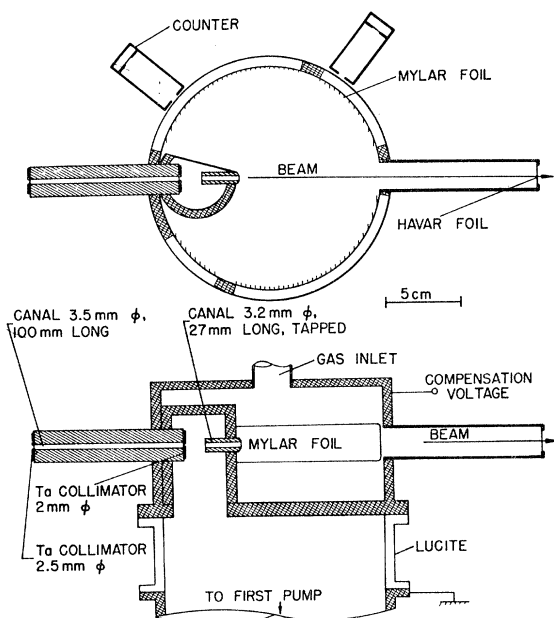


FIG. 1. The differentially pumped oxygen-gas target. The target shown here in vertical and horizontal views is mounted in a 60-cm scattering chamber and aligned optically. The Mylar foil windows are 0.5-mg cm^{-2} thick, and the beam exit Havar foil 2 mg cm^{-2} . The pressure in the target was 2 Torr and above the first pump, pumping the differential section, about 6×10^{-4} Torr. The high-voltage connection was made and the target pressure was measured at the wide gas-inlet tube.

(2) Further measurements were taken using a differentially pumped oxygen-gas target shown in Fig. 1. The entrance canals were 3.5 and 3.2 mm in diameter and a 1200-liter sec^{-1} diffusion pump was used on the differential section. The second canal, which was threaded inside in order to minimize scattering, served as a beam scraper. This system produced a target gas pressure of 2 Torr for a gas flow of 2.8 liters h^{-1} at STP. The geometry was such that no counter viewed

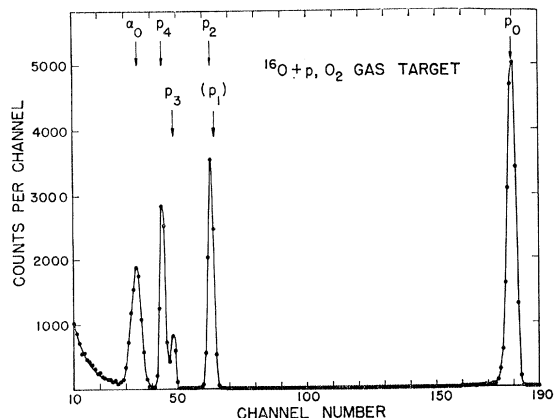


FIG. 2. Spectrum from the gas target obtained with a 1.5-mm thick silicon counter at 142° lab and $E_p = 11.28$ MeV. In order to maintain a low bias, the p_0 group is not completely stopped in the counter.

the 2-mg cm^{-2} Havar exit foil. Mylar foils 0.5 mg cm^{-2} in thickness in the walls acted both as windows for the scattered protons and as a means of reducing the scattering from the sides of the target chamber. The total energy loss of the beam in the gas-target region seen by the counters was always less than 700 eV, and the energy loss before entering this region was estimated to be less than 300 eV. Straggling is minimal under such conditions, and the main contribution of the target to the experimental resolution is the Doppler effect due to vibration in the oxygen molecule. The latter effect contributed about 700 eV to the over-all resolution. With this arrangement, the elastic and inelastic proton groups could be observed simultaneously at a number of angles. The counter biases were kept as low as possible and the beam was collected some distance downstream in order to reduce the neutron and γ -ray background in the

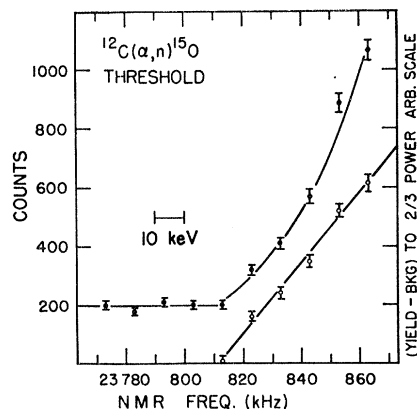


FIG. 3. The $^{12}\text{C}(\alpha, n)^{15}\text{O}$ reaction threshold. The full circles refer to the data. The open circles show these data raised to the two-thirds power after subtraction of the background. The points are plotted as a function of the nuclear magnetic resonance (NMR) frequency of the 90° beam analyzing magnet.

counters. The average angular spread accepted by the 54° , 90° , and 142° (lab) counters was $\pm 9.0^\circ$. A special collimator was used at 162° with an average spread of $\pm 5^\circ$.

Figure 2 illustrates the spectrum obtained. The p_1 and p_2 groups were never resolved with the counters. However, the p_1 group was known to be less than 5% of the p_2 group at 90° and 150° (lab), from the work on the spectrometer. At 54° (lab) the p_3 and p_4 groups were only partially resolved and the line shapes were used to separate the yields. At all angles the α_0 group from the $^{16}\text{O}(p, \alpha_0)^{13}\text{N}$ reaction occurred in the same region as the inelastic protons. The α_0 group was well separated at 142° (lab) as shown in Fig. 2. At 54° (lab) the α_0 group lay directly under the p_2 group so that the yield for the p_2 group presented in Fig. 5 contains α -particle counts.

The experimental resolution [full width at half-maximum (FWHM)] was measured to be less than 2 keV from the anomalies observed. In an effort to bring

the resolution nearer to the limit imposed by the target, part of the data was taken with a variable correction voltage applied to the insulated target chamber. The design allowed the target chamber potential to be varied by ± 2 kV by a signal derived from the image slits of the 90° analyzing magnet.

B. Energy Calibration Measurements

In order to determine accurately the positions of the two states a calibration of the analyzing magnet was made using the $^{12}\text{C}(\alpha, n)^{15}\text{O}$ reaction threshold and the resonance¹¹ in the $^{24}\text{Mg}(\alpha, \gamma)^{28}\text{Si}$ reaction at 3.1998 ± 0.001 MeV ($^4\text{He}^+$). The position of the $^{12}\text{C}(\alpha, n)^{15}\text{O}$ threshold is 11.346 ± 0.003 MeV from the 1964 mass heat before use. This procedure drastically reduced a table.¹² This reaction has been observed in the work of Nelson *et al.*,¹³ where positron counting of the 124-sec ^{15}O activity was used. A target chamber was constructed to allow a thick graphite target to be baked out to red

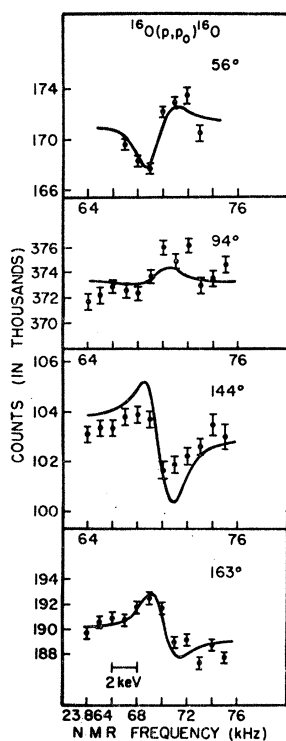


FIG. 4. The $^{16}\text{O}(p, p)^{16}\text{O}$ elastic scattering yields from the gas target at 56° , 94° , 144° , and 163° (c.m.). The points are plotted as a function of the NMR frequency of the 90° beam analyzing magnet. Only statistical errors are given. Also shown are theoretical curves from a phase-shift analysis. For the parameters used in these calculations, see Table I. The curves are arbitrarily normalized to the yields observed.

¹¹ A. Rytz, H. Staub, H. Winkler, and F. Zamboni, Nucl. Phys. 43, 229 (1963).

¹² J. H. E. Mattauch, W. Thiele, and A. H. Wapstra, Nucl. Phys. 67, 73 (1965).

¹³ J. W. Nelson, E. B. Carter, G. E. Mitchell, and R. H. Davis, Phys. Rev. 129, 1723 (1963).

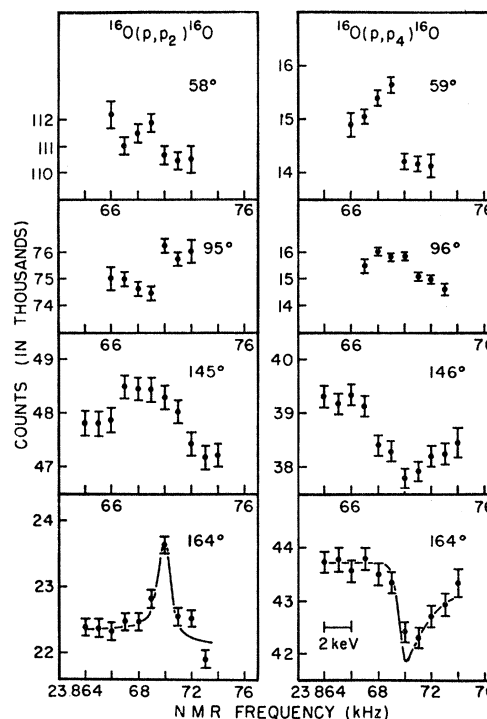


FIG. 5. The $^{16}\text{O}(p, p_2)^{16}\text{O}$ and $^{16}\text{O}(p, p_4)^{16}\text{O}$ inelastic-scattering yields from the gas target at various c.m. angles given in the figure. The points are plotted as a function of the NMR frequency of the 90° beam analyzing magnet and were taken at the same time as the elastic data shown in Fig. 4. Only statistical errors are given. The p_2 data points at 58° (c.m.) also contain the ground state alphas from $^{16}\text{O}(p, \alpha_0)^{13}\text{N}$ because the two groups could not be separated at this angle. It appears that the lowest $T = \frac{3}{2}$ state of ^{17}F is best located by observing the p_4 group near 54° (lab).

positron activity observed below threshold and attributed to $^{14}\text{N}(\alpha, n)^{17}\text{F}$. A further reduction in background was obtained by counting the two annihilation quanta in coincidence instead of the positrons. These improvements resulted in an increase in precision of the threshold from the ± 0.015 MeV of Nelson *et al.* to ± 0.005 MeV, as shown in Fig. 3. The narrow 3.1998-MeV resonance in the $^{24}\text{Mg}(\alpha, \gamma)^{28}\text{Si}$ reaction was observed with a semithick target and $^4\text{He}^+$ beam. The resonance was located to ± 0.002 MeV; however, this uncertainty is multiplied by four for the equivalent proton energy in the magnetic analyzer. Hence less weight was given to this measurement in the final result.

III. RESULTS

The elastic scattering data for the lowest $T = \frac{3}{2}$ state, recorded with the oxygen-gas target at 54° , 90° , and 162° (lab) are shown in Fig. 4. Also shown are theoretical curves which will be discussed in Sec. IV. Figure 5 shows data recorded at the same time in the inelastic channels to the 6.13- and 7.12-MeV states of ^{16}O . Data for the α_0 channel show no anomaly greater than 1% at 142° (lab) and 2% at 150° (lab). No

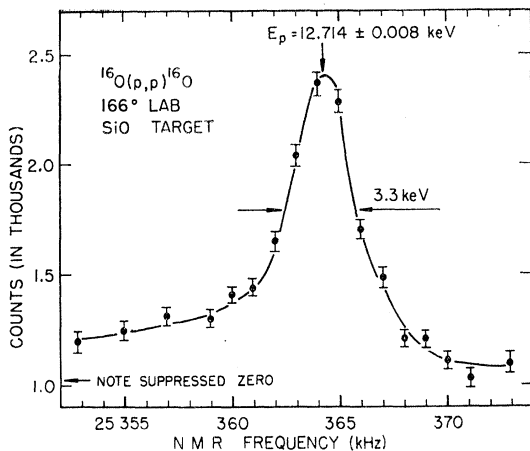


FIG. 6. The elastic scattering anomaly of the second $T=\frac{3}{2}$ state in ^{17}F at 166° (lab). The SiO target was about 1-keV thick and was covered with $8 \mu\text{g}/\text{cm}^2$ of gold on the back side in order to keep it at ground potential. Each datum point corresponds to $9 \mu\text{C}$. The counter solid angle was 2×10^{-3} sr.

anomaly greater than 2% was observed in p_3 at either 162° or 142° (lab). Data recorded at 150° (lab) for the p_2 and p_4 groups with the spectrometer are not shown. Fig. 6 shows the elastic scattering anomaly corresponding to the second $T=\frac{3}{2}$ state. The effect of the compensation voltage applied to the target in several of the runs was to increase the amplitudes of the anomalies. However, these data are not presented separately as they are not felt to be definitive.

The positions obtained for the two $T=\frac{3}{2}$ states are: $E_p=11.276 \pm 0.008$ and 12.714 ± 0.008 MeV, based on the $^{12}\text{C}(\alpha,n)^{15}\text{O}$ and $^{24}\text{Mg}(\alpha,\gamma)^{28}\text{Si}$ calibrations. The corresponding ^{17}F excitations are 11.202 ± 0.008 and 12.554 ± 0.008 MeV, respectively. The proton energy value for the second $T=\frac{3}{2}$ state given here supersedes an earlier value given by two of the authors¹⁴ and quoted by Marion.¹⁵ The errors are assigned from the accuracy of the 90° magnet calibration and the reproducibility of the position of the scattering anomalies. Both errors were of about equal significance. The results obtained are in good agreement with those of Adelberger and Barnes² and Van Bree and Temmer.¹⁶

IV. ANALYSIS AND DISCUSSION

The elastic scattering anomalies may reasonably be analyzed by the phase-shift method—particularly if complex phase shifts are allowed to take some account of the open nonelastic channels. The expression that was used in the analysis for the 11.20-MeV state is given by Goosman and Kavanagh,¹⁷ who kindly pro-

vided the computer program. The calculated anomalies were found to vary somewhat in shape and size over the range of scattering angles accepted by the counters at 142° , 90° , and 54° (lab) from the extended gas target. Therefore, anomalies calculated in steps of 1° were averaged with equal weight around the mean value of the angular acceptance of the counters. At 162° , where the counter collimators used were rather narrow, as pointed out in Sec. II A, no averaging procedure was used and the anomaly was calculated for 162° (lab) only. The averaging has a significant effect only for the 142° data, where the size of the anomaly to be expected at exactly 142° (lab) was reduced by about 20% due to the averaging over the range of scattering angles actually accepted by the 142° counter.

Apart from the phase shifts the following parameters enter the calculation of the anomalies: the orbital angular momentum of the protons l , J^π , Γ_{total} , and $\Gamma_{p_0}/\Gamma_{\text{total}}$ of the ^{17}F state, and the experimental resolution. Regardless of all other parameters only $l=1$ gives anomaly shapes consistent with the data for the lowest $T=\frac{3}{2}$ state at all four angles. Therefore this state has spin $\frac{1}{2}^-$ or $\frac{3}{2}^-$. A choice between the two values is difficult to make on the basis of elastic scattering measurements alone. Since Adelberger and Barnes² assigned a spin of $\frac{1}{2}^-$ to the state from stripping angular distributions, this value was chosen for the calculations. The experimental resolution was assumed to be Gaussian with a FWHM estimated from the data as a whole to be 1.5 to 2.0 keV. The runs using the compensation voltage are believed to have somewhat better resolution. However, no effort was made to treat these data separately, and a value of 2.0-keV FWHM was used for the calculations.

The nonresonant phase shifts were chosen to reproduce the elastic scattering angular distribution off resonance at $E_p=11.297$ MeV (Ref. 9), as shown in Fig. 7. This set also gave a ratio of the anomalies at 93° and 144° (c.m.) closest to the ratio observed. The

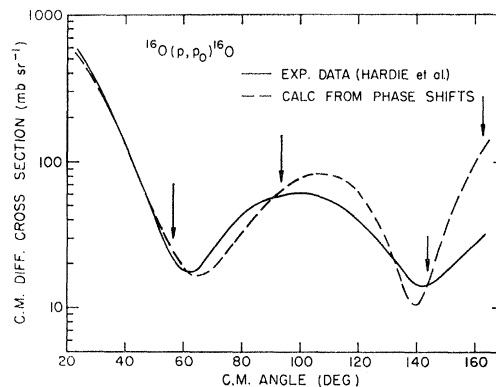


FIG. 7. The elastic scattering angular distribution as measured by Hardie *et al.*, at 11.297-MeV bombarding energy, and the fit to it obtained with the phase shifts given in Table I. The arrows indicate the angles at which the elastic scattering data of Fig. 4 were taken.

¹⁴ H. Winkler and C. S. Zaidins (private communication).

¹⁵ J. B. Marion, *Rev. Mod. Phys.* **38**, 660 (1966).

¹⁶ R. Van Bree and G. M. Temmer, *Bull. Am. Phys. Soc.* **12**, 518 (1967).

¹⁷ D. R. Goosman and R. W. Kavanagh, *Phys. Rev.* (to be published).

TABLE I. The parameters used in the calculations of the curves given in Fig. 4. Phase shifts are in radians. The expression used is given by Goosman and Kavanagh (Ref. 17). Note that the phase shifts depend on l but not on J . The curves are not sensitive to T_{total} , see text.

Nonresonant phase shifts:	$l=0$	$l=1$	$l=2$	$l=3$	$l=4$
Real:	+0.7	-0.15	-0.7	+0.33	0
Imag:	+0.1	0	+0.1	0	0

Parameters of the resonance:

$$l=1; J^{\pi}=\frac{1}{2}^{-}; \text{FWHM}=2000 \text{ eV}, \Gamma_{p_0}=40 \text{ eV}, \Gamma_{\text{total}}=130 \text{ eV}$$

phase shifts used in the calculations depend on l but not on J . Finally, a Γ_{p_0} was determined so as to fit the observed sizes of the anomalies. The result is $\Gamma_{p_0}=40$ eV. The error on this width is estimated to be $+20\%$ and -50% , on the basis of the uncertainties in the experimental resolution and the quality of the fits. Figure 4 shows the calculated curves and the data. The curves were normalized at each angle to the yield observed. The parameters used in the calculations are summarized in Table I.

An ambiguity arises in $\Gamma_{p_0}/\Gamma_{\text{total}}$. Once the FWHM of the experimental resolution and Γ_{p_0} are chosen, the size and shape of the calculated anomalies are relatively insensitive to Γ_{total} . The curves show no noticeable change for Γ_{total} between 100 and 500 eV. However, it is considered unlikely that $\Gamma_{p_0}/\Gamma_{\text{total}}$ is smaller than 0.2.

Note added in proof. Recent experiments have shown that $\Gamma_{p_0}/\Gamma_{\text{total}}$ is indeed smaller than 0.2. A preliminary value of $\Gamma_{p_0}/\Gamma_{\text{total}}=0.1\pm 0.05$ has been obtained by Adelberger *et al.*¹⁹ from $n-p$ coincidence work with the $^{15}\text{N}(^3\text{He},n)^{17}\text{F}^*$ reaction. This result is in agreement with the work of Esterlund *et al.*²⁰ on the delayed proton emission from ^{17}Ne . Therefore, the width of the state is less than about 800 eV. The anomalies observed in the elastic and in the inelastic p_2 and p_4 groups are comparable in size, and measurements of Hensley and

Barnes¹⁸ on the analog state in ^{17}O indicate that the ratio $\Gamma_{\gamma}/\Gamma_{\text{total}}$ is small. There is also no observable anomaly in the α_0 channel. With this restriction on $\Gamma_{p_0}/\Gamma_{\text{total}}$, an upper limit of about 200 eV can be placed on the width of the state. A $\frac{3}{2}^{-}$ -spin assignment would give even lower values of Γ_{p_0} and Γ_{total} .

No analysis was attempted for the inelastic data (Fig. 5), although the resonance is strongest in p_2 at 164° and p_4 at 59° and 164° (c.m.). Solid curves are drawn in by eye at 164° c.m. where the shapes are confirmed by the spectrometer data.

A phase-shift analysis was also performed on some elastic scattering data from the second $T=\frac{3}{2}$ state, not shown here. This analysis clearly required $l=1$, which together with the alternatives of $\frac{3}{2}^{-}$ or $\frac{5}{2}^{-}$ for the spin as found by Adelberger and Barnes, determines the spin of this state to be $\frac{3}{2}^{-}$.

The second $T=\frac{3}{2}$ state is narrow ($\Gamma < 3$ keV) and can be observed easily at backward angles in the elastic scattering from a SiO target as shown in Fig. 6. It may therefore prove to be a useful accelerator calibration point, since it can be determined better than thresholds at higher proton energies. An absolute calibration of the proton energy producing this scattering anomaly to about ± 1 keV is highly desirable. The state is also useful as a check on accelerator resolution. The first $T=\frac{3}{2}$ state, while more difficult to find, could be a useful test of unusually high resolution.

ACKNOWLEDGMENTS

The authors wish to thank E. G. Adelberger and C. A. Barnes for suggesting this experiment, D. R. Goosman for the use of his phase-shift program, and T. Lauritsen for helpful discussions.

¹⁸ D. C. Hensley and C. A. Barnes (private communication).

¹⁹ E. G. Adelberger, C. L. Cocke, and C. N. Davids (private communication).

²⁰ R. A. Esterlund, R. McPherson, A. M. Poskanzer, and P. L. Reeder, Phys. Rev. **156**, 1094 (1967).